



## Imaging of the GI tract by QDs loaded heparin–deoxycholic acid (DOCA) nanoparticles

Zehedina Khatun<sup>a</sup>, Md. Nurunnabi<sup>a</sup>, Kwang Jae Cho<sup>b,\*</sup>, Yong-kyu Lee<sup>a,\*</sup>

<sup>a</sup> Department of Chemical and Biological Engineering, Korea National University of Transportation, Chungbuk 380-702, Republic of Korea

<sup>b</sup> Department of Otolaryngology, Head & Neck Surgery, The Catholic University of Korea, College of Medicine Uijeongbu St. Mary's Hospital, Kyunggi-Do 480-717, Republic of Korea

### ARTICLE INFO

#### Article history:

Received 21 December 2011

Accepted 5 July 2012

Available online 16 July 2012

#### Keywords:

Heparin

Oral delivery

GI tract

*In vivo* imaging

Near-IR QDs

### ABSTRACT

This study presents an approach to deliver non invasive, near-IR imaging agent using oral delivery system. Low molecular weight heparin (LMWH)–deoxycholic acid (DOCA)/(LHD) nanoparticles formed by a self-assembly method was prepared to evaluate their physicochemical properties and oral absorption *in vitro* and *in vivo*. Near-IR QDs were prepared and loaded into LHD nanoparticles for imaging of the gastro-intestinal (GI) tract absorption. Q-LHD nanoparticles were almost spherical in shape with diameters of 194–217 nm. The size and fluorescent intensity of the Q-LHD nanoparticles were stable in 10% FBS solution and retained their fluorescent even after 5 days of incubation. Cell viability of Q-LHD nanoparticles maintained in the range of 80–95% for 24 h incubation. No damage was found in tissues or organs during animal experiments. The *in vivo* oral absorption of Q-LHD was observed in SKH1 mice for 3 h under different doses. From the results, we confirmed that Q-LHD was absorbed mostly into the ileum of small intestine containing intestinal bile acid transporter as observed in TEM and molecular imaging system. Our designed nanoparticles could be administered orally for bio-imaging and studying the bio-distribution of drug.

© 2012 Elsevier Ltd. All rights reserved.

### 1. Introduction

Low molecular weight heparin (LMWH) is a naturally occurring glycosaminoglycan that is widely known as an anticoagulant agent (Chen et al., 2009; Klement, Du, Berry, Andrew, & Chan, 2002; Lehman & Frank, 2009). LMWH is also used for initial therapy regarding venous thromboembolism, which is a common complication of cancer patients (Lee, 2009; Streiff, 2006, 2009). Over the last few decades, it has been found that LMWH can inhibit cancer progression through anti-angiogenesis and tumor metastasis. The most interesting aspect of using LMWH is that several clinical applications have evidenced no severe toxicity such as bleeding and heparin-induced thrombocytopenia (Kuderer, Ortel, & Francis, 2009; Simka & Urbanek, 2009). However, the application of LMWH is possible only through the intravenous (IV) route to avoid its poor absorption in the intestine; high molecular weight, negatively charged structure, and high water solubility (Kim et al., 2006; Lee, Nam, Shin, & Byun, 2001; Motlekar, Srivenugopal, Wachtel, & Youan, 2005). Various types of approaches have been studied such as enteric coatings, liposomes, and enhancers for the oral delivery of heparin (Lee, Kim, & Byun, 2000; Lee et al., 2001). Some researchers have also studied the oral delivery of LMWH by coupling with

bile acids, such as deoxycholic acid (DOCA) and taurocholic acid (TCA) (Lee et al., 2006, 2009). Previously, we reported that the LMWH–DOCA conjugate (LHD) has shown excellent absorption profiles after oral administration to rodents and monkeys (Kim, Lee, Kim, et al., 2007; Lee et al., 2007; Park, Jeon, Kim, Al-Hilal, Jin, et al., 2010; Park, Jeon, Kim, Al-Hilal, Moon, et al., 2010; Park, Kim, et al., 2010). The intestinal absorption of heparin derivatives appeared due to the coupling of DOCA molecules. This DOCA could promote intestinal absorption, increase hydrophobic properties of heparin and interaction between heparin derivative and bile acid transporters of intestinal membrane (Kim et al., 2005).

Highly fluorescent nano-sized quantum dots (QDs) (5–10 nm) made of inorganic semiconductor materials (Cd, Te, and Se) possess several unique optical properties that are ideal for *in vivo* imaging (Pan & Feng, 2009; Smith & Nie, 2008). Near-infrared (near-IR) QDs (emissions of 650–950 nm) have been found to be more effective than visible QDs (emissions of 450–650 nm) for *in vivo* (especially) deep tissue and organ imaging (Jamieson et al., 2007; Nurunnabi, Cho, Choi, Huh, & Lee, 2010). For the biological application of QDs, the surfaces of hydrophobic QDs have been modified by some biocompatible polymers such as PEG (polyethylene glycol), mPEG (methoxy polyethylene glycol), PLGA (poly(lactic-co-glycolic acid)), and PAA (poly(acrylic acid)) (Aldeek et al., 2011; Su et al., 2010). QDs have been used for sentinel lymph node mapping, tumor targeting, tumor angiogenesis imaging, and metastatic cell tracking (Kim et al., 2011; Lee et al., 2010; Zhou et al., 2010). Non-invasive

\* Corresponding authors. Tel.: +82 43 841 5238; fax: +82 43 841 5220.

E-mail addresses: [entckj@catholic.ac.kr](mailto:entckj@catholic.ac.kr) (K.J. Cho), [leeyk@ut.ac.kr](mailto:leeyk@ut.ac.kr) (Y.-k. Lee).

imaging is the most promising technique for early diagnosis of cancer, angiogenesis and the bio-distribution of drugs (Gao et al., 2010; Louie, 2010).

In this study, we prepared near-IR QDs loaded LHD nanoparticles for noninvasive images of the GI tract. The Q-LHD nanoparticles were also characterized to measure the size, morphology, stability, and loading efficacy. Finally, the designed Q-LHD formulation was orally administered in mice and the absorption of LHD through the bile acid transporter was evaluated with molecular imaging system (KMIS), and TEM. We proposed that LHD nanoparticles can be used as an oral imaging agent delivery for bio-imaging.

## 2. Materials and methods

### 2.1. Materials

Low molecular-weight heparin (Fraxiparine or LMWH, MW: 5000 Da) was obtained from Mediplex Corp. (Seoul, Korea). Sodium deoxycholic acid (DOCA), dimethyl formamide (DMF), triethyl amine (TEA), 4-nitrophenylchloroformate, absolute ethanol (EtOH), formamide, 4-methylmorpholine, ethylenediamine, dimethyl sulfoxide (DMSO), *N*-hydroxysuccinimide (NHS), *N,N'*-dicyclohexylcarbodiimide (DCC), trioctylphosphine oxide (TOPO), hexadecylamine (HAD), cadmium oxide, selenium powder, and dodecanoic acid were obtained from Sigma–Aldrich, Co. (St. Louis, MO). Caco-2 cells were collected from the Korea cell bank (Seoul, Korea). Cell culture reagents including fetal bovine serum (FBS) and Minimum essential medium (MEM), were purchased from Sigma–Aldrich, Co. (St. Louis, MO). Sodium bicarbonate ( $\text{NaHCO}_3$ ) was purchased from OCI Co., Ltd. (Seoul, Korea). *N*-2-hydroxyethyl-piperazine-*N'*-4-butanesulfonic acid (HEPES) was purchased from Biosesang (Seoul, Korea) and penicillin–streptomycin was purchased from Gibco BRL (Carlsbad, CA). 3-(4,5-Dimethylthiazol-2-yl)-2,5-diphenyl tetrazolium bromide (MTT) was purchased from Amresco, Inc. (Solon, OH). A Coatest Heparin FXa assay kit was purchased from Chromogenix (Milano, Italy).

### 2.2. Synthesis of the LHD conjugates

The chemical conjugates of LMWH and DOCA were synthesized by conjugating the hydroxyl group of DOCA with the carboxylic group of LMWH according to our previous method (Kim et al., 2006; Lee et al., 2001; Motlekar et al., 2005). For amination of deoxycholic acid (DOCA, 0.77 mmol) in 5 mL DMSO was reacted with 4-nitrophenyl chloroformate (4-NPC, 3.86 mmol) and triethylamine (4.63 mmol) for 6 h at room temperature. After reaction, the precipitant was removed by 0.45  $\mu\text{m}$  filter membrane. The filtrate was extracted with 25 mL ethyl acetate and 25 mL water. The crude product from aqueous solution was washed with ethyl acetate three times, and then DOCA carbonate was obtained as a powder type after freeze-drying. To obtain aminated DOCA, DOCA carbonate was reacted with 4-methylmorpholine (1.10 mmol) and ethylenediamine (0.05 mmol) overnight at room temperature. The product was concentrated by rotary evaporation and then precipitated by adding acetonitrile.

For preparation of the LMWH–DOCA conjugate, LMWH (0.02 mmol) was dissolved in water and adjusted to pH 5.0 by adding 0.1 M HCl solution. The solution was mixed with EDAC (0.04 mmol), NHS (0.04 mmol), and aminated DOCA (0.044 mmol). After 30 min, the mixture was dialyzed (MWCO: 2000) against water to remove unreacted NHS, EDAC, and aminated DOCA. The final product, LMWH–DOCA, was obtained and stored at 4 °C after freeze-drying. The dried LMWH–DOCA conjugate was analyzed by  $^1\text{H}$  NMR and FT-IR (Bruker, Germany). Values for  $^1\text{H}$  NMR of

heparin ( $\text{D}_2\text{O}$ ) were:  $\delta$  5.38 [H1 of glucosamine residue (A)],  $\delta$  5.04 [H1 of iduronic acid residue (I)],  $\delta$  4.84 [I-5],  $\delta$  4.36–4.23 [A-6],  $\delta$  4.12–4.40 [I-3],  $\delta$  4.08j [I-4],  $\delta$  4.02 [A-5],  $\delta$  3.78 [I-2],  $\delta$  3.71 [A-4],  $\delta$  3.65–3.69 [A-3],  $\delta$  3.24 [A-2]. Values for  $^1\text{H}$  NMR of aminated DOCA ( $\text{D}_2\text{O}$ ) were:  $\delta$  1.2–1.9 [m, five and six rings of DOC, 1H],  $\delta$  2.1–2.3 [m,  $\text{CH}_3$  of DOC, 1H],  $\delta$  3.15 [d, 12R-OH of DOC, 2H],  $\delta$  8.0 [H of CONH]. Values of  $^1\text{H}$  NMR of LMWH–DOCA conjugates ( $\text{D}_2\text{O}$ ) were:  $\delta$  1.2–1.9 [m, five and six rings of DOCA, 1H],  $\delta$  3.24–5.38 [A or I of heparin],  $\delta$  8.0–8.2 [H of CONH of LMWH–DOCA]. The feed mole ratio of LMWH and DOCA was controlled to 1:2.6, 1:4, 1:6.7, and 1:13.3, respectively.

### 2.3. Characterization of the LHD conjugates

The LHD conjugation was confirmed by the formation of amide bonds between the carboxylic groups of heparin and the amine group of DOCA using FT-IR and  $^1\text{H}$  NMR. For FT-IR, the LHD conjugates were scanned as a solid powder. The spectra were Fourier transformed after 32 scans were acquired with a resolution of  $2\text{ cm}^{-1}$ . The chemical conjugation of LMWH and DOCA was proved by  $^1\text{H}$  NMR of the amide bond formed between the carboxylic groups of LMWH with the amine group of DOCA- $\text{NH}_2$ . For the  $^1\text{H}$  NMR (JNM-AL400, Jeol Ltd., Akishima, Japan) study, the LHD conjugates (20 mg) were dissolved in  $\text{D}_2\text{O}$  solvent. The size distribution, shape and morphology of the Q-LHD particles were examined using dynamic light scattering (DLS) (ELS-Z, Otsuka Electronics Co., Ltd., Tokyo) and a JEM-100CX TEM (JEOL, Tokyo), respectively. For TEM examination, one drop of Q-LHD was placed on a thin copper grid. The fluorescent intensities and emission spectra of Q-LHD were investigated by a Varioskan flash (Thermo Scientific, NY).

### 2.4. Preparation of QDs-loaded LHD nanoparticles (Q-LHD)

For loading of QDs into LHD nanoparticles, 20 mg of LHD was dissolved in 2.5 mL of formamide; then, different amounts of QDs solution (0.110  $\mu\text{g}/\text{mL}$  in chloroform) was added into the conjugate solution. The mixture was vigorously stirred to facilitate the hydrophobic QDs to be loaded in the core of the LHD micelles. Chloroform was evaporated due to stirring in an open flask after overnight stirring, and the remaining chloroform was evaporated under reduced pressure. The solution was dialyzed against water for 2 days to exchange the organic solvent with an aqueous solution. The free unloaded hydrophobic QDs became aggregated in the aqueous medium and precipitated. The solution was filtered by a hydrophobic filter to remove the precipitated QDs. Finally, the product was dried for 48 h by a freeze dryer.

### 2.5. Stability of LHD and Q-LHD

To investigate the stability of LHD and Q-LHD nanoparticles, we measured the changes in the fluorescent intensity and average size of Q-LHD nanoparticles in an aqueous solution and serum over time at three different pH (5, 7 and 9) in 0.1 M PBS buffer, respectively. LHD and Q-LHD nanoparticles were separately dispersed into each pH buffer solution (1 mg/mL) for 2 h. The average diameter of the LHD and Q-LHD nanoparticles was then measured using a DLS (ELS-Z, Otsuka Electronics Co., Ltd., Tokyo). The stability of LHD and Q-LHD nanoparticles in the presence of serum (10% (v/v) in PBS and FBS) was also measured to evaluate non-specific binding with proteins. To minimize interference by large molecules in FBS, the serum solution was filtered using a 0.45  $\mu\text{m}$  filter membrane. The LHD and Q-LHD nanoparticles were then incubated in the FBS solution for five days, and any change in size was monitored.

## 2.6. *In vitro* cytotoxicity study

The cytotoxicities of the LHD conjugates, water-soluble QDs, and Q-LHD nanoparticles were examined through human colon cancer cell line of Caco-2 cells (Korea cell bank). The Caco-2 cells were cultured at 37 °C in a humidified atmosphere containing 5% CO<sub>2</sub> in a MEM medium with 10% fetal calf serum. The cells (5 × 10<sup>4</sup> cells/mL) grown as a monolayer were harvested by 0.25% trypsin–0.03% EDTA solution. The cells (200 μL) in their respective media were seeded in a 96-well plate and pre-incubated for 24 h before the assay. The cell viability of the Caco-2 cell lines was evaluated in the different groups by the MTT colorimetric assay kit. The Caco-2 cells were placed in the 96-well plates and incubated for 24 h. After suction, the complete medium and the sample were placed and again incubated in the referred condition. MTT solution aliquots at 5 mg/mL in PBS were prepared followed by culture incubation with this solution at 5% in the culture medium for 4 h in an incubator with a moist atmosphere of 5% CO<sub>2</sub> and 95% air at 37 °C. Afterwards, 100 μL of the MTT solubilizing solution was added to each well. After smooth and slow shaking for 15 min, the MTT colorimetric assay absorbance was measured at a 570 nm wavelength with a Varioskan flash and was directly proportional to the cell viability. The cell viability was expressed as a percentage. It was calculated by the following equation:

$$\text{cell viability (\%)} = \left( \frac{\text{sample absorbance}}{\text{control absorbance}} \right) \times 100$$

## 2.7. Oral absorption and imaging study

To observe the absorption sites of the Q-LHD nanoparticles, SKH1 mice were used, each weighing about 20–25 mg. After 12 h of fasting, near-IR QD-loaded LHD nanoparticles were administered at different doses (2.5 mg/kg and 5 mg/kg) by oral gavage. After 8 h of administration, the mice were dissected and their tissues of the small intestinal parts were collected and washed in PBS buffer for 30 min. The tissue from each part was homogenized with a homogenizer for 3 min and centrifuged at 4000 rpm for 5 min. The supernatant part of the extracts was collected and the fluorescence was measured by a Varioskan flash.

To measure the anti-Factor Xa (FXa) activity, the blood samples were diluted with human normal plasma (100 μL), anti-thrombin III (ATIII) solution (100 μL), and DI water and incubated at 37 °C for 3 min. Further, FXa (100 μL) was added to the solution, and the solution was again incubated for 30 s. A substrate (200 μL) was then added to the solution, and again the solution was incubated for 3 min. Finally, the reaction was ended by adding 300 μL of 20% acetic acid. The oral absorption of Q-LHD was calculated from the absorbance at 405 nm.

**Statistics.** Statistical analysis was done using ANOVA.  $p < 0.05$  was accepted as statistically significant. Error bars represent standard deviation.

## 3. Results and discussion

### 3.1. Synthesis and characterization of LHD

We synthesized LMWH–DOCA conjugates for oral absorption imaging by linking the LMWH with DOCA (Fig. 1). Conjugation between the carboxyl groups of LMWH and the amine groups of DOCA was confirmed by the presence of signals at  $\delta$  8.0–8.2 ppm in the <sup>1</sup>H NMR spectrum. The selective modification of C3–OH was conducted by a suitable protected side chain of C12–OH group. It also took advantage of the known reactivity order of the two

hydroxyl groups in DOC structure, C3–OH > C12–OH (Geldern et al., 2004). The coupling ratio of DOCA molecules with LMWH was varied according to the feed mole ratio of DOCA and LMWH. We found that five moles of DOCA were coupled with LMWH with maximum (Table 1). The purities of each conjugates were analyzed by liquid chromatography (LC). All products were found over 79% purity and 43% yield. Among various conjugates, LHD6.7 was selected for loading of QDs due to its highest yield and purity. LHD conjugates formed self-assembled nanoparticles in an aqueous medium because of their lipophilic property. The average particle size of the nanoparticles was about 185 nm in diameter. The average size of the LHD particles decreased with an increasing amount of conjugated DOCA due to the increased hydrophobic interaction among the DOCA molecules in aqueous medium. Critical micelles concentration (CMC) also varied from 0.001 to 0.005 mg/mL among the different formulations due to variation in the number of coupled DOCA molecules (the data are not shown). The CMC data has shown that the CMC decreased according to increasing coupling amount of DOCA.

### 3.2. Loading of near-IR QDs into LHD conjugates

Near-IR QDs has been synthesis according to our previous methods (Kim et al., 2011). After the conjugation and characterization of LHD conjugates, hydrophobic, highly luminescent near-IR QDs (wavelength of 661 nm) was loaded into the nanoparticles by solid dispersion methods. In brief, the LHD6.7 conjugate was dissolved in formamide solution and stirred until the solution become clear. Chloroform containing QDs solution was added with the LHD6.7 solution and stirred overnight at ambient conditions. The mixture was dialyzed again DI water for 48 h to remove the organic solvents. The loaded amount of hydrophobic near-IR QDs and the florescent intensity of QD-loaded LHD (Q-LHD) nanoparticles were varied by varying the amount of near-IR QDs added to the solution. The loading efficiency of Q-LHD series was changed from 56% to 81%, indicating that strong hydrophobic interaction between near-IR QDs and conjugated DOCA in LHD. The result also indicated that the encapsulated QDs endow the increased hydrophobic property and dense nanoparticle structure as shown in TEM (Fig. 2A). The QDs loaded LHD nanoparticles with spherical shape and uniform size distribution were obtained as shown in ELS data (Table 1). After loading of QDs in LHD6.7, the average size distribution was varied from 194 nm to 217 nm in diameter.

### 3.3. Stabilities of Q-LHD nanoparticles

The stabilities of LHD6.7 and Q-LHD5 against 10% serum and pH changes were analyzed by measuring the change in the size and fluorescent intensity of LHD6.7 and Q-LHD5 nanoparticles (Fig. 2B–D). After each LHD6.7 and Q-LHD5 was dispersed in PBS buffer with different pH (5, 7 and 9) for 2 h, the sizes were measured by using ELS. Our results demonstrated that the pH change had a minimal effect on the stability of LHD6.7 and Q-LHD5. For example, the mean diameter of Q-LHD5 was around 195, 220 and 225 nm in pH 5, 6 and 7, respectively. We then examined the change of the size distribution and fluorescent intensity of Q-LHD5 for 5 days of incubation in the 10% serum (FBS). As shown in Fig. 2D, the average size was increased a little to 230 nm in diameter, indicating a relative stability in 10% serum for 5 days. This result may indicate no severe leakage of QDs from LHD5 nanoparticle. We believe that LHD nanoparticles have excellent solubility and stability, suggesting a role as a probe in biological systems imaging. To the best of our knowledge, this is the first method for delivery of imaging agent through orally in combined with LHD nanoparticles.

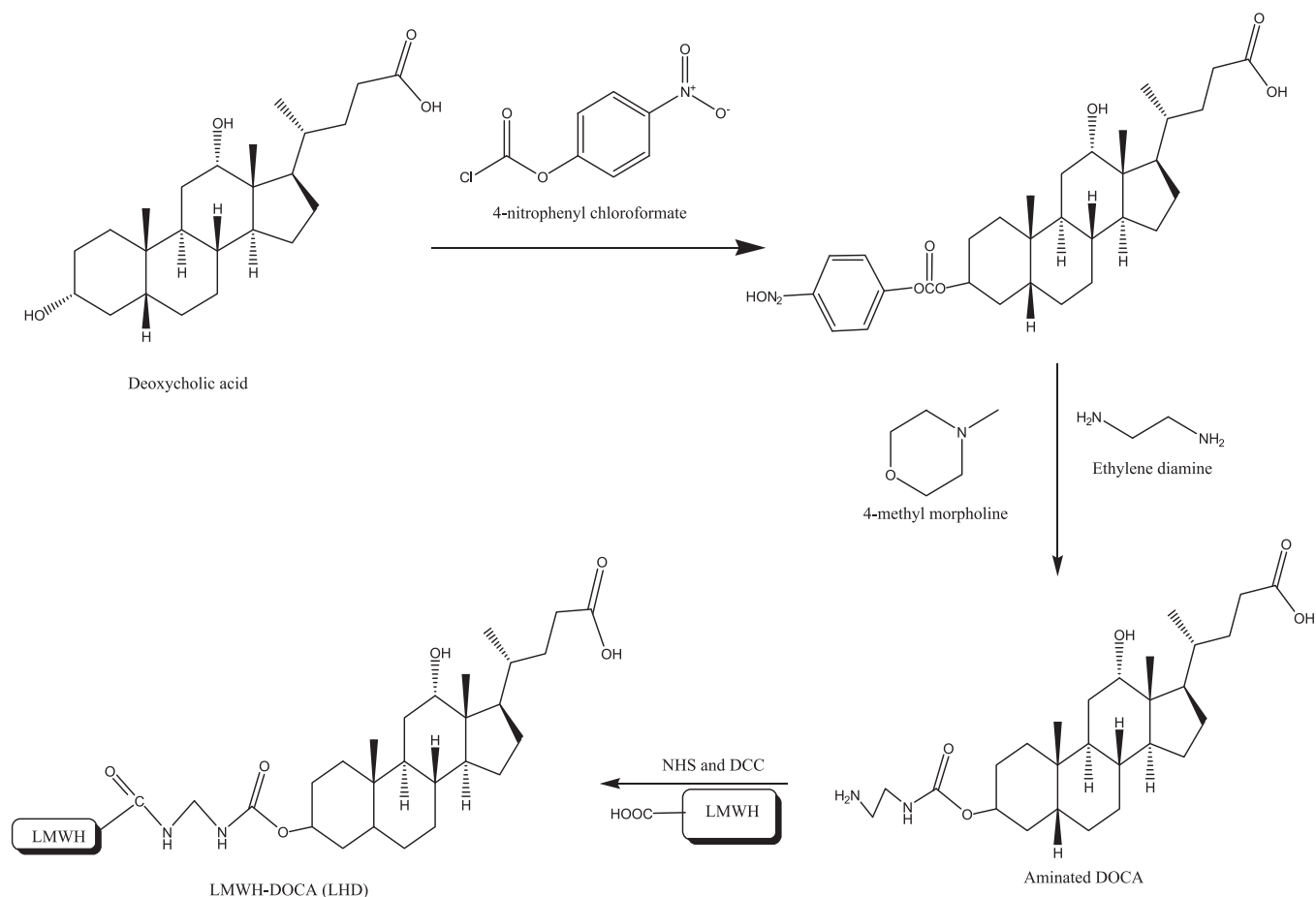


**Fig. 1.** Conjugation of LMWH and DOCA. An orally active LHD conjugate was synthesized by forming an amide bond between the aminated group of DOCA and the carboxyl group of LMWH.

### 3.4. *In vitro* cytotoxicity study

To assess the cytotoxicity of Q-LHD5, a Caco-2 cell line was used. Blank LHD nanoparticles, water-soluble QDs, and Q-LHD5 nanoparticles were incubated with cells with different concentrations (0.1  $\mu\text{g}/\text{mL}$ , 1  $\mu\text{g}/\text{mL}$ , 10  $\mu\text{g}/\text{mL}$ , 50  $\mu\text{g}/\text{mL}$  and 100  $\mu\text{g}/\text{mL}$ ) for different time durations (24 h and 48 h). Overall, MTT assay indicates that cytotoxic effects were not significant because cell viability was still in the range from 80% to 95% for 24 h incubation. After 48 h incubation, the cell viability of the Caco-2 cells was still maintained over 60% after treating of Q-LHD5, no observing  $\text{IC}_{50}$  values in the range of 0.1–100  $\mu\text{g}/\text{mL}$  (Fig. 3A and B). Also, according to statistics, the differences among the groups were not significant because  $p$ -values among the groups were greater than 0.05. Therefore, we believe that the effect of Q-LHD5

on the cell viability and metabolic activities was not numerically significant.

### 3.5. Imaging of oral absorption

Blood samples were collected by retro orbital pulses using capillary tube at 30 min, 60 min, 120 min, and 180 min after the oral administration of Q-LHD5 nanoparticles (2.5 mg/kg and 5 mg/kg). After collecting plasma samples, we measured plasma concentration and fluorescent intensity of Q-LHD5 nanoparticles. The results showed that the Q-LHD5 nanoparticles were rapidly absorbed in the intestine and found in the blood circulation at both doses (Fig. 4A). The maximum plasma concentrations ( $C_{\text{max}}$ ) were  $0.82 \pm 0.19$  and  $0.95 \pm 0.3$  IU/mL for 2.5 mg/kg and 5 mg/kg, respectively, where as  $T_{\text{max}}$  was 120 min for both dosages. The effective

**Table 1**  
Characterization of LHD and Q-LHD to measure the coupling ratio, loaded QDs conc., yield, particle size and purity.

Sample name	Feed molar ratio (heparin:DOCA)	Coupling molar ratio (heparin:DOCA)	Loaded QDs conc. ( $\mu\text{g}/\text{mL}$ )	Yield (%)	Particle size (nm)	Purity (%)
LHD2.6	1:2.6	1:1.20	–	43.1	$205.5 \pm 40$	91.87
LHD4.0	1:4	1:2.18	–	54.5	$186.9 \pm 35$	79.24
LHD6.7	1:6.7	1:4.28	–	64.0	$187.6 \pm 32$	97.49
LHD13.3	1:13.3	1:5.79	–	43.5	$176.2 \pm 23$	82.25
Q-LHD1	1:6.7	1:4.28	0.110	56.2	$194.1 \pm 33$	–
Q-LHD2	1:6.7	1:4.28	0.165	60.4	$199.4 \pm 37$	–
Q-LHD3	1:6.7	1:4.28	0.220	69.0	$206.1 \pm 42$	–
Q-LHD4	1:6.7	1:4.28	0.275	77.1	$212.6 \pm 48$	–
Q-LHD5	1:6.7	1:4.28	0.330	81.0	$217.1 \pm 43$	–

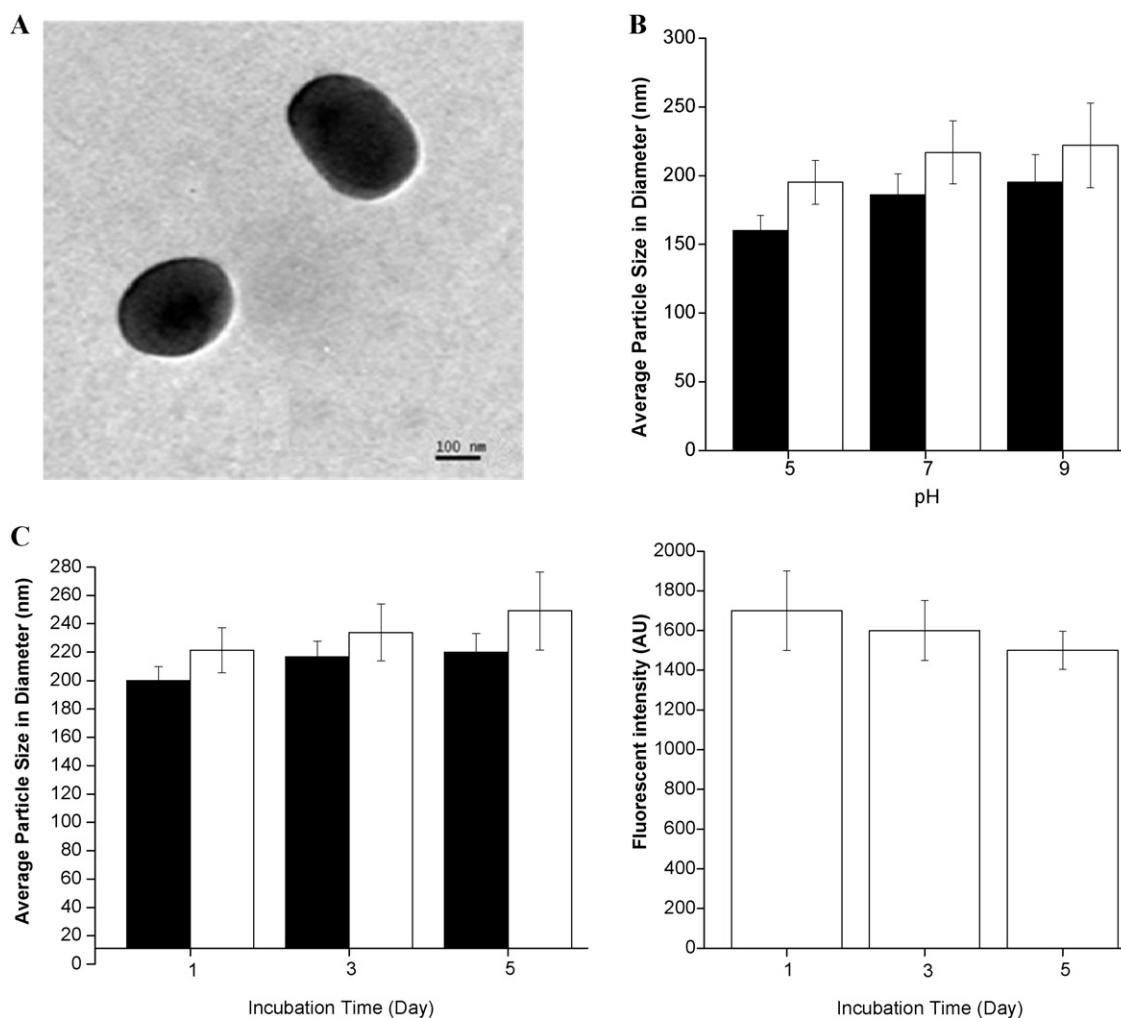


**Fig. 2.** TEM image and stabilities of Q-LHD5 nanoparticles. TEM observation (A) of Q-LHD5 and average particle size distribution of LHD (■) and Q-LHD5 (□) at different pH conditions (B). Average particle size distribution (C) and fluorescent intensity (D) of Q-LHD5 in 10% FBS solutions for 5 days.

area under the curve (AUC) was  $24.49 \pm 6.0$  and  $37.38 \pm 11.0$ , respectively. AUC also varied as the dose varied. In our previous study, we found that the effective maximum concentration ( $E_{max}$ ) increased as the quantity of conjugated DOCA increased (Park, Kim,

et al., 2010). The data on the oral absorption of Q-LHD5 showed a similar trend, which indicated that the loaded QDs had no effect on the oral absorption (Fig. 4B). In our previous study, it was proved that a higher coupling ratio of DOCA with LMWH increased the oral

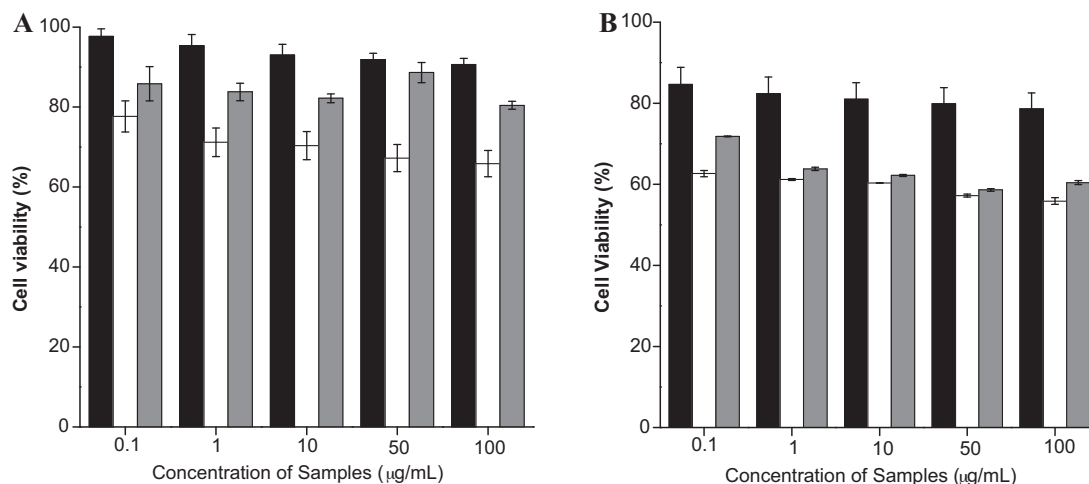


**Fig. 3.** Cell viability of Caco-2 cells after treating LHD6.7 (■), water-soluble QDs (□) and Q-LHD5 (■) nanoparticles for 24 and 48 h, respectively. The data are plotted as mean  $\pm$  SD ( $n = 3$ ).

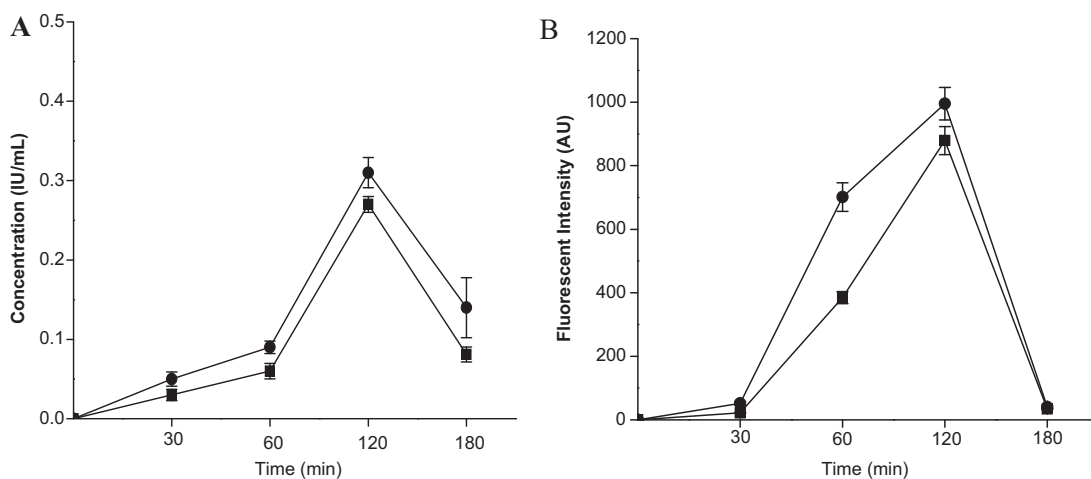


**Fig. 4.** Plasma concentration (A) and fluorescent intensity (B) after oral administration of Q-LHD5 nanoparticles in mice. The dosage of Q-LHD5 nanoparticles in mice was controlled to 2.5 (■) and 5 mg/kg (●).

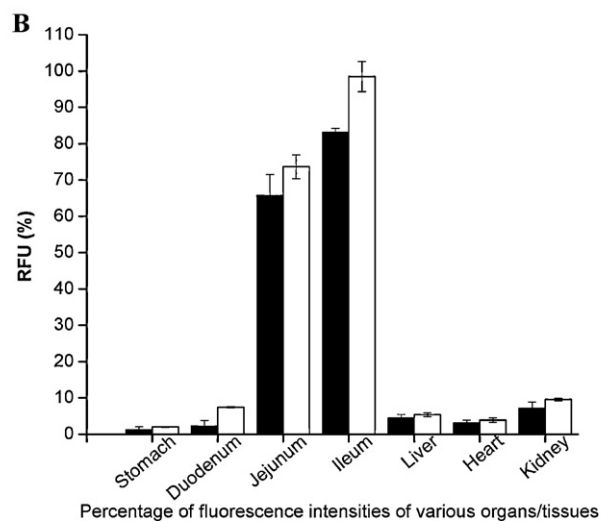
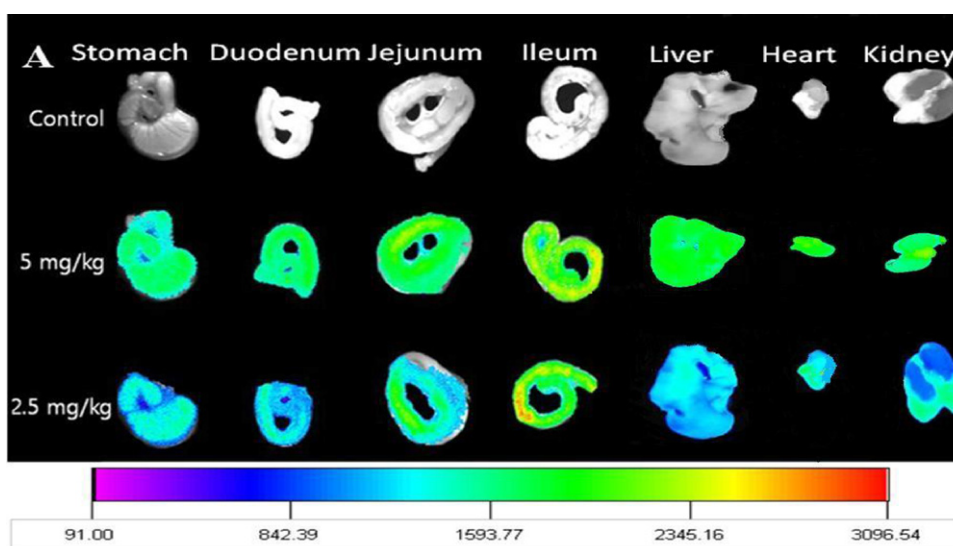


**Fig. 5.** (A) *Ex vivo* fluorescent images of the GI tract and organs isolated at 8 h post oral administration of Q-LHD5 nanoparticles. (B) Quantification of the *ex vivo* fluorescent intensity of Q-LHD5 nanoparticles. The dosage of Q-LHD5 nanoparticles was controlled to 2.5 (■) and 5 mg/kg (□). The mice treated with only PBS buffer set as a control ( $n=3$ ).

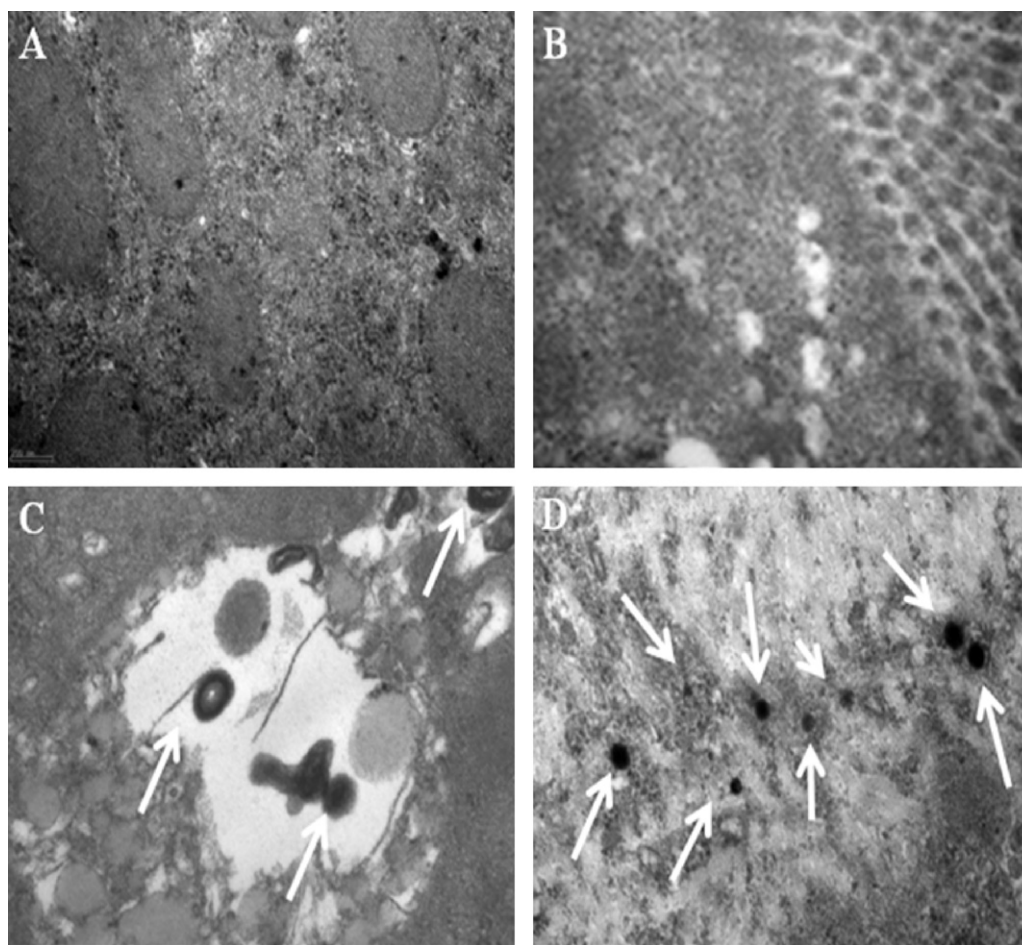


**Fig. 6.** TEM images of isolated (A) stomach, (B) duodenum, (C) jejunum and (D) ileum after oral administration of Q-LHD5 nanoparticles. White arrows indicate the presence of Q-LHD5 nanoparticles in the tissues of the ileum and jejunum. Scale bar represents 100 nm.

absorption of LHD compared with a lower coupling ratio of DOCA (Park, Jeon, Kim, Al-Hilal, Jin, et al., 2010; Park, Jeon, Kim, Al-Hilal, Moon, et al., 2010).

The mice were also dissected after the oral administration of different doses of Q-LHD5 nanoparticles to get images of the isolated GI tract and organs such as the liver, heart, and kidneys by KMIS for visualizing the absorption site. The KMIS images showed the strongest fluorescent signal in the ileum, indicating that nanoparticles were absorbed mainly through the ileum due to the presence of large numbers of the intestinal bile acid transporter (IBAT) (Kim, Lee, Lee, et al., 2007). On the contrary, few amounts of nanoparticles were absorbed in the stomach, duodenum, and jejunum where the fluorescent signal was weaker than in the ileum (Fig. 5A), and sensitive organs such as the liver and kidneys contained higher fluorescence as compared to the heart. The absorption percentages were measured by a Variskan flash after extraction of the organs to get the exact, absorbed quantities of Q-LHD5 nanoparticles at different parts of the small intestine and stomach. The fluorescent intensities of the Q-LHD5 nanoparticles were 62% and 75% for the 2.5 mg/kg dose, and 65% and 90% for the 5 mg/kg dose in the jejunum and ileum, respectively (Fig. 5B). The fluorescent intensities of the nanoparticles in the stomach and duodenum were negligible, viz., below 1% and 2% for 2.5 mg/kg and below 1.5% and 3% for 5 mg/kg, respectively. The maximum absorption amounts of Q-LHD5 nanoparticles were found in the jejunum and ileum (62–90% of the total absorbed Q-LHD5 nanoparticles) in the case of both the 2.5 mg/kg and 5 mg/kg doses, whereas a negligible amount of Q-LHD5 nanoparticle absorption was found in the stomach and

duodenum (1.5–3% of the total absorbed Q-LHD5 nanoparticles). The GI tract was then observed by TEM to observe the presence of Q-LHD5 nanoparticles in each region. The data confirmed that the maximum number of particles was absorbed by the ileum (Fig. 6D) (Kim, Lee, Lee, et al., 2007). Few numbers of particles were found in the jejunum (Fig. 6C), and no particles were found in the stomach and duodenum (Fig. 6A and B). Quantitative analysis of the fluorescence intensity indicated that the amount of Q-LHD5 accumulated at the absorption site was approximately 6–10 folds higher than that of other organs. These results are in good agreement with TEM data (Fig. 6).

The effective use of nanoparticles for biomedical imaging would be visualized when *in vivo* biodistribution is clearly understood. From our results, the fluorescent signals at the specific area were much stronger than in the other organs, which allow for a clear discrimination between organs. This high specific absorption of Q-LHD nanoparticles might be due to a combination of bile acid transporter mediated absorption as well as adequate carrier system. Overall, these results demonstrated that Q-LHD nanoparticles are absorbed at ileum of small intestine and show potential for use as an imaging agent for oral absorption study.

#### 4. Conclusions

Near-IR QDs loaded LHD nanoparticles was successfully prepared for noninvasive images of the GI tract. The designed Q-LHD formulation was orally administered in mice and the absorption of LHD through the bile acid transporter was evaluated with

molecular imaging system (KMIS) and TEM. Q-LHD nanoparticles were absorbed at ileum of small intestine and show potential for use as an imaging agent for oral absorption study. The designed carrier for oral delivery imaging has been proven to be safe and effective for imaging GI absorption with a constant oral absorption and pharmacokinetics profile.

## Acknowledgements

This research was supported by Basic Science Research Program through the National Research Foundation of Korea (NRF) funded by the Ministry of Education, Science and Technology (2010-0021427).

## References

- Aldeek, F., Mustin, C., Balan, L., Roques-Carmes, T., Fontaine-Aupart, M., & Schneider, R. (2011). Surface-engineered quantum dots for the labeling of hydrophobic microdomains in bacterial biofilms. *Biomaterials*, *32*, 5459–5470.
- Chen, M.-C., Wong, H.-S., Lin, K.-J., Chen, H.-L., Wey, S.-P., Sonaje, K., et al. (2009). The characteristics, biodistribution and bioavailability of a chitosan-based nanoparticulate system for the oral delivery of heparin. *Biomaterials*, *30*, 6629–6637.
- Gao, J., Cehn, K., Xie, R., Xie, J., Yan, Y., Cheng, Z., et al. (2010). In vivo tumor-targeted fluorescence imaging using near-infrared non-cadmium quantum dots. *Bioconjugate Chemistry*, *21*, 604–609.
- Geldern, V. T. W., Tu, N., Kym, P. R., Link, J. T., Jae, H. S., Lai, C., et al. (2004). Liver-selective glucocorticoid antagonists: A novel treatment for type 2 diabetes. *Journal of Medicinal Chemistry*, *17*, 4213–4230.
- Jamieson, T., Bakhshi, R., Petrova, D., Pocock, R., Imani, M., & Seifalian, A. M. (2007). Biological applications of quantum dots. *Biomaterials*, *28*, 4717–4732.
- Kim, J. S., Cho, K. J., Tran, T. H., Nurunnabi, M., Moon, H. T., Hong, S. M., et al. (2011). In vivo NIR imaging with CdTe/CdSe quantum dots entrapped in PLGA nanospheres. *Journal of Colloid and Interface Science*, *353*, 363–371.
- Kim, S. K., Kim, K., Lee, S., Park, K., Park, J. H., Kwon, I. C., et al. (2005). Evaluation of absorption of heparin–DOCA conjugates on the intestinal wall using a surface plasmon resonance. *Journal of Pharmaceutical and Biomedical Analysis*, *39*, 861–870.
- Kim, S. K., Lee, D. Y., Kim, C. Y., Nam, J. H., Moon, H. T., & Byun, Y. (2007). A newly developed oral heparin derivative for deep vein thrombosis: Non-human primate study. *Journal of Controlled Release*, *123*, 155–163.
- Kim, S. K., Lee, D. Y., Lee, E., Lee, Y.-k., Kim, C. Y., Moon, H. T., et al. (2007). Absorption study of deoxycholic acid–heparin conjugate as a new form of oral anti-coagulant. *Journal of Controlled Release*, *120*, 4–10.
- Kim, S. K., Vaishali, B., Lee, E., Lee, S., Lee, Y.-k., Kumar, T. S., et al. (2006). Oral delivery of chemical conjugates of heparin and deoxycholic acid in aqueous formulation. *Thrombosis Research*, *117*, 419–427.
- Klement, P., Du, Y. J., Berry, L., Andrew, M., & Chan, A. K. C. (2002). Blood-compatible biomaterials by surface coating with a novel antithrombin–heparin covalent complex. *Biomaterials*, *23*, 527–535.
- Kuderer, K. M., Ortel, T. L., & Francis, C. W. (2009). Impact of venous thromboembolism and anticoagulation on cancer and cancer survival. *Journal of Clinical Oncology*, *27*, 4902–4911.
- Lee, A. Y. Y. (2009). Anticoagulation in the treatment of established venous thromboembolism in patients with cancer. *Journal of Clinical Oncology*, *27*, 4895–4901.
- Lee, P.-W., Hsu, S.-H., Tsai, J.-S., Chen, F.-R., Huang, P.-J., Ke, C.-J., et al. (2010). Multifunctional core–shell polymeric nanoparticles for transdermal DNA delivery and epidermal Langerhans cells tracking. *Biomaterials*, *31*, 2425–2434.
- Lee, E., Kim, Y.-S., Bae, S. M., Kim, S. K., Jin, S., Chung, S. W., et al. (2009). Polyproline-type helical-structured low-molecular weight heparin (LMWH)–taurocholate conjugate as a new angiogenesis inhibitor. *International Journal of Cancer*, *124*, 2755–2765.
- Lee, Y.-k., Kim, S. K., & Byun, Y. (2000). Oral delivery of new heparin derivatives in rats. *Pharmaceutical Research*, *17*, 1259–1264.
- Lee, D. Y., Kim, S. Y., Kim, Y. S., Son, D. H., Nam, J. H., Kim, I. S., et al. (2007). Suppression of angiogenesis and tumor growth by orally active deoxycholic acid–heparin conjugate. *Journal of Controlled Release*, *118*, 310–317.
- Lee, Y.-k., Kim, S. K., Lee, D. Y., Lee, S., Kim, C.-Y., Shin, H.-C., et al. (2006). Efficacy of orally active chemical conjugate of low molecular weight heparin and deoxycholic acid in rats, mice and monkeys. *Journal of Controlled Release*, *111*, 290–298.
- Lee, Y.-k., Nam, J. H., Shin, H.-c., & Byun, Y. (2001). Conjugation of low-molecular-weight heparin and deoxycholic acid for the development of a new oral anticoagulant agent. *Circulation*, *104*, 3116–3120.
- Lehman, C. M., & Frank, E. L. (2009). Laboratory monitoring of heparin therapy: Partial thromboplastin time or anti-Xa assay? *LabMedicine*, *40*, 47–51.
- Louie, A. (2010). Multimodality imaging probes: Design and challenges. *Chemical Reviews*, *110*, 3146–3195.
- Motlekar, N. A., Srivenugopal, K. S., Wachtel, M. S., & Youan, B.-b. C. (2005). Oral delivery of low-molecular-weight heparin using sodium caprate as absorption enhancer reaches therapeutic levels. *Journal of Drug Targeting*, *13*, 573–583.
- Nurunnabi, M., Cho, K. J., Choi, J. S., Huh, K. M., & Lee, Y.-k. (2010). Targeted near-IR QDs-loaded micelles for cancer therapy and imaging. *Biomaterials*, *31*, 5436–5444.
- Pan, J., & Feng, S.-S. (2009). Targeting and imaging cancer cells by Folate-decorated, quantum dots (QDs)-loaded nanoparticles of biodegradable polymers. *Biomaterials*, *30*, 1176–1183.
- Park, J. W., Jeon, O. C., Kim, S. K., Al-Hilal, T. A., Jin, S. J., Moon, H. T., et al. (2010). High antiangiogenic and low anticoagulant efficacy of orally active low molecular weight heparin derivatives. *Journal of Controlled Release*, *148*, 317–326.
- Park, J. W., Jeon, O. C., Kim, S. K., Al-Hilal, A. T., Moon, H. T., & Byun, Y. (2010). Anticoagulant efficacy of solid oral formulations containing a new heparin derivative. *Molecular Pharmaceutics*, *7*, 836–843.
- Park, J. W., Kim, S. K., Al-Hilal, A. T., Jeon, O. C., Moon, H. T., & Byun, Y. (2010). Strategies for oral delivery of macromolecule drugs. *Biotechnology and Bioengineering*, *15*, 66–75.
- Simka, M., & Urbanek, T. (2009). Anti-metastatic activities of heparins. *Journal of Cancer Molecules*, *5*, 3–8.
- Smith, A. M., & Nie, S. (2008). Minimizing the hydrodynamic size of quantum dots with multifunctional multidentate polymer ligands. *Journal of the American Chemical Society*, *130*, 11278–11279.
- Streff, M. B. (2006). Long-term therapy of venous thromboembolism in cancer patients. *Journal of the National Comprehensive Cancer Network*, *4*, 903–910.
- Streff, M. B. (2009). Diagnosis and initial treatment of venous thromboembolism in patients with cancer. *Journal of Clinical Oncology*, *27*, 4889–4894.
- Su, Y., Hu, M., Fan, C., He, Y., Li, Q., Li, W., et al. (2010). The cytotoxicity of CdTe quantum dots and the relative contributions from released cadmium ions and nanoparticle properties. *Biomaterials*, *31*, 4829–4834.
- Zhou, Y., Shi, L., Li, Q., Jiang, H., Lv, G., Zhao, J., et al. (2010). Imaging and inhibition of multi-drug resistance in cancer cells via specific association with negatively charged CdTe quantum dots. *Biomaterials*, *31*, 4958–4963.